

Imbalanced charge carrier mobility and Schottky junction induced anomalous current-voltage characteristics of excitonic PbS colloidal quantum dot solar cells

Lilei Hu^a, Andreas Mandelis^{a,b,*}, Xinzheng Lan^b, Alexander Melnikov^a, Sjoerd Hoogland^b, Edward H. Sargent^b

^a Center for Advanced Diffusion-Wave and Photoacoustic Technologies (CADIPT), Department of Mechanical and Industrial Engineering, University of Toronto, Toronto, Ontario, Canada M5S 3G8

^b Edward S. Rogers Sr. Department of Electrical and Computer Engineering, University of Toronto, Toronto, Ontario, Canada M5S 3G4

ARTICLE INFO

Article history:

Received 12 March 2016

Received in revised form

6 June 2016

Accepted 7 June 2016

Available online 15 June 2016

Keywords:

Colloidal quantum dot solar cells

Photovoltaic

Exciton

Hopping mobility

Schottky diode

Heterojunction

ABSTRACT

Anomalous current-voltage (I-V) characteristics, as reported with increasing frequency, can significantly compromise the energy conversion efficiency of colloidal quantum dot (CQD) solar cells. This paper applied a purely hopping transport model rather than the traditional Schottky-diode equation to interpret the anomalous I-V curves measured in CQD solar cells with a structure: ITO/ZnO/PbS-TBAI QD/PbS-EDT QD/Au. Anomalous I-V curves were found at temperatures below 300 K. A double-diode-equivalent electric circuit was developed for the quantitative analysis of these anomalous I-V curves, yielding multiple hopping transport parameters, such as hopping diffusivity, diffusion length, mobility, and lifetime. Quantitative analysis revealed that the imbalanced charge carrier mobility in the carrier transport (PbS-TBAI) and extraction (PbS-EDT) layers, as well as the existence of a reverse Schottky diode at the PbS-EDT/Au interface, played key roles in the formation of the anomalous I-V curves. Furthermore, charge-transfer (CT) states, located at the ZnO/PbS-TBAI interface, were found to reduce the CQD solar cell open-circuit voltage through radiative and non-radiative recombination of excitons. A modified Einstein equation was also validated, further proving the presence of a Schottky barrier and pointing to a rate determining interface for the I-V behaviors of our solar cells.

© 2016 Elsevier B.V. All rights reserved.

1. Introduction

Colloidal quantum dots (CQDs) have attracted much attention in the past few years due to two major advantages: a) their solution fabrication process that provides possibilities for low-cost, light weight, flexible, and roll-to-roll processed electronics [1–6]; and b) tunable optical and electrical properties through feasible quantum dot size control [7–10]. As a result, CQD-based solar cells have emerged as one of most promising photovoltaic devices ever since they were first reported in 2005 [11]. In the meantime, their power conversion efficiency (PCE) and in-air stability have been significantly improved under intensive development; for example, recently researchers have successfully demonstrated respectable long-term air-stability (~5 months) for a double-QD layer solar

cell architecture [12]. Our group was also successful in driving the highest current CQD solar cell PCE to 10.7% [13]. Both of these milestones are crucial in evaluating its commercial potential, further encouraging the photovoltaics community. Specifically, there are three dominant CQD solar cell architectures: Schottky-diode, heterojunction, and CQD sensitized solar cells [14]. Compared with the other two architectures, for Schottky-diode based CQD solar cells, given a short-circuit current density (J_{sc}), device efficiency is diminished by the lower Fill Factor (FF) and open-circuit voltage (V_{oc}) which are due to a poor energy barrier for hole injection into the electron-extraction electrode [14]. Furthermore, in CQD sensitized solar cells, charge transport is facilitated due to the micrometer-thick matrix, however, light absorption efficiency is reduced as a consequence of this thin layer of light absorber on a high surface area electrode [14]. In comparison, heterojunction based CQD solar cells are much better with respect to the final device energy conversion efficiency, as they can simultaneously maximize FF , V_{oc} and I_{sc} as well as light absorption efficiency through proper material energy band engineering and

* Corresponding author at: Center for Advanced Diffusion-Wave and Photoacoustic Technologies (CADIPT), Department of Mechanical and Industrial Engineering, University of Toronto, Toronto, Ontario, Canada M5S 3G8.

E-mail address: mandelis@mie.utoronto.ca (A. Mandelis).

optimization of the light-absorption layer thickness [14]. Exciton hopping transport in CQD solar cells involves exciton diffusion and dissociation distinct from charge transport mechanisms which govern conventional inorganic silicon cells [7]. However, most studies of CQD solar cells to-date are based on the classical Schottky diode equation that was derived under the assumption of continuous energy band semiconductor systems where electron-hole pairs dissociate immediately upon their generation and travel at high charge mobility. Crystalline Si is representative of these photovoltaic materials whereas CQD and organic solar cells are excluded from that category [15,16]. Würfel, et al. demonstrated that the Schottky equation cannot be applied to low-mobility materials in the way it is used for inorganic solar cells, and device parameters extracted from the Schottky equation such as ideality factor, series resistances and shunt resistance lack real physical meaning [17] and provide very limited assistance toward the optimization of device fabrication. In comparison, material parameters including carrier mobilities, diffusion length, lifetime, diffusivity, and trap states offer more important information for solar cell device structure optimization, starting with selection of materials. Unfortunately, in common with organic photovoltaic materials, CQDs constitute low carrier mobility photovoltaic materials and have high exciton binding energy, both impediments to improving solar efficiency in a straightforward manner. In summary, a full understanding of charge carrier transport mechanism within CQD devices is lacking.

Another impediment to solar cell device efficiency is the formation of a Schottky junction at the CQD/anode interface which forms an electric field with direction opposite to that of the light incidence. This Schottky junction causes holes to accumulate at the CQD/anode interface [16,18], thereby reducing the surface recombination velocity (SRV) as observed in organic photovoltaic devices [19]. All of these adverse processes handicap hole extraction at the anode and lead to low solar conversion efficiency. An experimental consequence of hole accumulation is the formation of anomalous (including S-shaped) current-voltage (I-V) curves, which have been reported for heterojunction CQD solar cells with increasing frequency [12,15,20]. Nevertheless, the origins of the formation of these anomalous I-V curves have not been well understood, nor have they been exploited toward designing higher performance solar cells. Wang et al. [21] attributed them to the electron accumulation effect induced by an exciton blocking layer. Wagenpahl et al. [19] found the reduction of hole-associated surface recombination velocities could also give rise to S-shaped I-V curves. One approach to study S-shaped I-V curves is through fitting experimental data to theoretical electric circuit models. However, although Romero et al. [22] developed equivalent electric circuit models that can quantitatively simulate three kinds of I-V curves in terms of forward and reverse diodes, they did not consider actual physical mechanisms. Here we analyze the temperature-dependent I-V characteristics using a double-diode electric circuit model and a hopping transport model to explain their origins. In addition, performance factors of our device architecture are discussed with improvement recommendations.

2. CQD solar cell fabrication and I-V measurement

PbS CQDs were prepared following our previous reports [23,24]. Briefly, oleic acid (4.8 mmol), PbO (2.0 mmol) and 1-octadecene (ODE, 56.2 mmol) were mixed and heated to 95 °C under vacuum. This was followed by the injection of bis(trimethylsilyl) sulphide and ODE at a high temperature of 120 °C. After cooling, the PbS CQDs were successively precipitated and redispersed using acetone and toluene, respectively. The products were stored in a nitrogen glovebox for further surface passivation

treatments. CQD solar devices fabricated in this manner have the structure of ITO/ZnO/PbS-TBAI QD/PbS-EDT QD/Au which has been demonstrated by two groups to be stable for ca. 5 months [12], and at least 1 month [13], respectively. S-shaped I-V curves at room temperature for a CQD solar cell with this structure were also reported by Chuang et al. [12] but were not well-understood in terms of physical optoelectronic processes. Devices were fabricated in air through a typical solution process [12,23,25]. TBAI and EDT denote tetrabutylammonium iodide and 1, 2-ethanedithiol, respectively. They are exchange-ligands for PbS CQDs to passivate quantum dot surface trap states and adjust the interdot distance which determines the coupling strength between two neighboring dots. The exciton transition energy (effective band gap) of PbS QD was measured in a solid CQD nanolayer to be ca. 1.4 eV. In the fabrication process, a ca.100-nm ZnO nanoparticle layer was spin-coated onto a clean glass substrate with a pre-deposited ITO electrode of 145 nm thickness. PbS QD layers were deposited through a layer-by-layer spin-coating process, after which a TBAI solution (10 mg/ml in methanol) was applied to the substrate for 30 s, followed by successive methanol rinse-spin steps. An EDT solution (0.01 vol% in acetonitrile) and acetonitrile were used for the deposition of the PbS-EDT nanolayer. As examined by scanning electron spectroscopy, the final thicknesses of PbS-TBAI and PbS-EDT were ca. 200 nm and 50 nm, respectively. In addition, a 120-nm-thick Au anode was evaporated on the top of PbS-EDT. Fig. 1 shows a schematic of the fabricated CQD solar cell. Its energy diagram is shown in Fig. 2 which illustrates that, under illumination, excitons generated in PbS-TBAI dissociate into free electron and hole carriers through interdot coupling strength and the electric field at the heterojunction interface. Free-electrons are swept onto the cathode within the depleted area. In addition, because of the energy barrier formed at the PbS-TBAI/PbS-EDT interface, electrons are blocked from flowing to the anode which can significantly increase I_{sc} and V_{oc} [12,25]. Unfortunately, as will be discussed later, such architecture leads to the formation of a Schottky barrier in PbS-EDT, which prevents holes from being extracted to the external Au anode, resulting in hole accumulation and formation of an electric field with reverse direction to the forward field in the main heterojunction diode (PbS-TBAI/ZnO). In the following discussion, for the sake of clarification, the subscript h refers to the heterojunction diode (ZnO/PbS-TBAI) and s refers to the Schottky diode (PbS-EDT/Au). Fig. 3 shows the equivalent circuit: two diodes with opposite electric field directions representing heterojunction and Schottky diode, respectively.

The homojunction formed at the PbS-TBAI/PbS-EDT interface gives rise to an electric field with forward direction, same as that of the heterojunction, but its strength is diminished by the reverse Schottky barrier because of the low PbS-EDT layer thickness (50 nm). Therefore, to simplify the analysis and improve

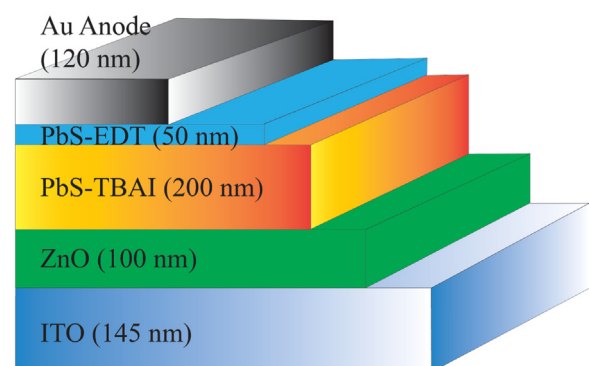


Fig. 1. Schematic of double-layer CQD solar cell with the structure: ITO/ZnO/PbS-TBAI QD/PbS-EDT QD/Au.

دانلود مقاله



<http://daneshyari.com/article/77501>



- ✓ امکان دانلود نسخه تمام متن مقالات انگلیسی
- ✓ امکان دانلود نسخه ترجمه شده مقالات
- ✓ پذیرش سفارش ترجمه تخصصی
- ✓ امکان جستجو در آرشیو جامعی از صدها موضوع و هزاران مقاله
- ✓ امکان پرداخت اینترنتی با کلیه کارت های عضو شتاب
- ✓ دانلود فوری مقاله پس از پرداخت آنلاین
- ✓ پشتیبانی کامل خرید با بهره مندی از سیستم هوشمند رهگیری سفارشات